Geomechanics and Engineering, *Vol. 7, No. 3 (2014) 279-295*
DOI: http://dx.doi.org/10.12989/gae.2014.7.3.279

Time-dependent behaviour of interactive marine and terrestrial deposit clay

Xiaoping Chen [*1], Qingzi Luo [1] and Qiujuan Zhou [2]

[1] *MOE Key Laboratory of Disaster Forecast and Control in Engineering, College of Science and Engineering, Jinan University, Guangzhou, 510632, PR China*
[2] *Guangdong Technical College of Water Resources and Electric Engineering, Guangzhou, 510635, PR China*

(*Received September 24, 2013, Revised May 20, 2014, Accepted May 30, 2014*)

Abstract. A series of one-dimensional consolidation tests and triaxial creep tests were performed on Nansha clays, which are interactive marine and terrestrial deposits, to investigate their time-dependent behaviour. Based on experimental observations of oedometer tests, normally consolidated soils exhibit larger secondary compression than overconsolidated soils; the secondary consolidation coefficient (C_α) generally gets the maximum value as load approaches the preconsolidation pressure. The postsurcharge secondary consolidation coefficient (C_α') is significantly less than C_α. The observed secondary compression behaviour is consistent with the C_α/C_c concept, regardless of surcharging. The C_α/C_c ratio is a constant that is applicable to the recompression and compression ranges. Compared with the stage-loading test, the single-loading oedometer test can evaluate the entire process of secondary compression; C_α varies significantly with time and is larger than the C_α obtained from the stage-loading test. Based on experimental observations of triaxial creep tests, the creep for the drained state differs from the creep for the undrained state. The behaviour can be predicted by a characteristic relationship among axial strain rate, deviator stress level and time.

Keywords: secondary consolidation coefficient; creep; time-dependent; interactive marine and terrestrial deposit clay; laboratory

1. Introduction

Natural soft clays exhibit significant time-dependent deformations in both laboratory and in-situ conditions. They are rate-controlled by the viscous-like resistance of the soil structure and are important in geotechnical problems. In the design of foundations on soft ground, the time-dependent deformation behaviour must be calculated to control postconstruction settlement, including the long-term settlement of structures on compressible ground and deformations of earth structures. Time-dependent deformations have been extensively investigated via simple stress and deformation states, such as one-dimensional and triaxial test conditions in a laboratory. The one-dimensional consolidation test (oedometer test) is generally performed to determine primary compression (occurs during an increase in effective vertical pressure) and secondary compression (a delayed settlement at a constant effective vertical pressure). Due to the confining ring-imposed

*Corresponding author, Professor, E-mail: chenxp@jnu.edu.cn

http://www.techno-press.org/?journal=gae&subpage=7 ISSN: 2005-307X (Print), 2092-6219 (Online)

zero lateral strain on the test specimen, the secondary compression in the test is considered to be volumetric creep. Mesri (Mesri 1973, 2003, Mesri and Castro 1987, Mesri and Godlewski 1977, Mesri *et al*. 1997) summarized the identification and characterization of primary consolidation and secondary consolidation in the oedometer condition and noted that the secondary compression coefficient C_α is directly related to the compression index C_c in marine clay and peat deposits. The relationship between C_α and C_c was confirmed and investigated by other researchers (Al-Shamrani 1998, Santagata *et al*. 2008, Tong *et al*. 2012, Badv and Sayadian 2012, Jesmani *et al*. 2012). Deng *et al*. (2012) performed low-pressure and high-pressure oedometer tests on Boom clay and examined the influencing factors of C_α. The triaxial creep test generally focuses on the stress-level dependency of strains that develop over time, i.e., the creep in this test is reflects the development of time-dependent shear and/or volumetric strain interrelationship under constant effective stress. Due to the drainage condition during creep, the creep behaviour in the triaxial test is defined as drained creep and undrained creep. Singh and Mitchell (1968) defined the parameter m for various normally consolidated clays, which is represented by a slope of the straight line in the logarithm of strain rate and time. Additional studies presented the results of triaxial creep tests on marine clays, and the relationship among the strain rate of axial and/or volumetric, deviator stress level and time is an interesting research area with a long history (Bishop and Lovenbury 1969, Arulanandan *et al*. 1971, Tavenas *et al*. 1978, Tian *et al*. 1994, Fodil *et al*. 1997, Sheahan *et al*. 1996, Miao *et al*. 2008, Zhu and Yin 2001).

The majority of studies on time-dependent behaviour are derived from slightly overconsolidated and normally consolidated marine deposit clays. This paper investigates the time-dependent deformation behaviour of interactive marine and terrestrial deposits, which exhibited significant soil structure and stress-path dependence (Chen *et al*. 2008, Zeng and Chen 2009). A series of oedometer tests and triaxial creep tests were performed on intact samples, and the behaviours of secondary compression and triaxial creep were analyzed. The law of C_α/C_c and the rate process parameter m were presented.

2. Soil sampling and index property

Intact samples investigated in this paper were obtained from the depth range of 6.0-8.0 m below the ground surface, a relatively homogenous layer, which is located at a marine site in Nansha of Guangzhou (refer to Fig. 1). The deposit is typical interactive marine and terrestrial clay that is referred to as Nansha clay; it belongs to the Q_4W series in the Pearl River Delta (Qiao *et al*. 2002). All samples were obtained using a thin-walled sampler, which had been carefully sealed and transported from the site. These samples were black grey in colour and consisted of a mixture of clay, silt and sand. By X-ray diffraction analysis, the main clay minerals were identified as illite and kaolinite with a minor amount of chlorite and smectite; the silt and fine-sand fraction contained quartz and muscovite. The particle size analysis test showed that the composition is 50%-60% clay (< 5 μm), with approximately 30% colloid fraction (< 2 μm), 4% sand (> 75 μm) and 6%-8% organic matter. The grain size distribution is shown in Fig. 2(a). Photomicrographs of freeze-dried samples revealed a flocculent link structure with a weak directionality of flake clay mineralogy (refer to Fig. 2(b)). With the infrastructure development in this area, this type of soil is frequently encountered in underground earth structures. The study of time-dependent deformation behaviour is prompted by the practical need.

The geotechnical properties of the investigated clay, which are characterized by high compressibility and low shear strength as a result of a high initial water content and void ratio, are

Fig. 1 Sampling site of Nansha clay

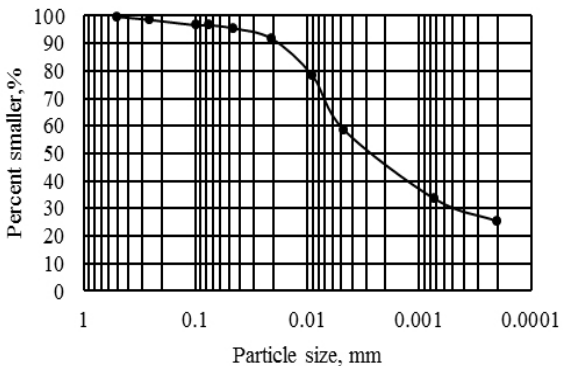

(a) Particle size distribution curves

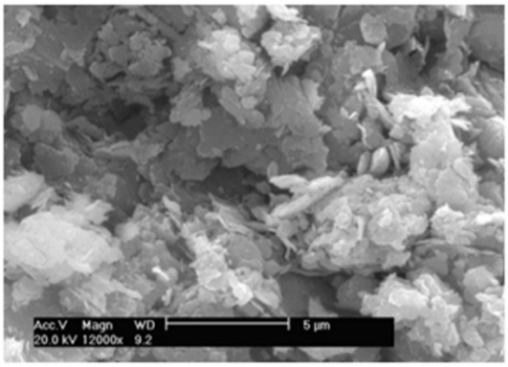

(b) Scanning electron microphotographs

Fig. 2 Particle size distribution and photomicrographs of Nansha clay

summarised in Table 1. The initial permeability was slightly higher than general marine clay due to the silty fine sand fraction. The liquid limits w_L ranged from 37.4%-59.8%, and the plasticity indices I_p ranged from 16.5-34.1. According to the Chinese National Standard, Code for the Investigation of Geotechnical Engineering (GB 50021-2001), it is categorized as a clay with high plasticity.

3. Laboratory testing techniques

3.1 Oedometer test

The intact sample was trimmed to a diameter of 61.8 mm and a height of 20 mm. After trimming equipment was installed in the cell with a minimum of disturbance, drainage was allowed at the top and bottom. The loading was applied suddenly in the test, and the duration of each pressure was prescribed prior to the test. All tests were performed in a temperature-controlled room (24°C ± 1) to minimise the effect of temperature on the consolidation tests.

Three types of loading methods were performed in this study:

Table 1 Geotechnical properties of Nansha clay

Index		Statistical samples	Average (extreme values)
Water content	w_0/(%)	278	56.34 (45.6-83.5)
Density	ρ/(g·cm^{-3})	147	1.62 (1.50-1.87)
Void ratio	e_0	74	1.32 (1.01-1.96)
Specific gravity	d_s	50	2.63 (2.57-2.69)
Liquid limit	w_L/(%)	101	47.5 (37.4-59.8)
Plasticity index	I_p	101	24.1 (16.5-34.1)
Coefficient of permeability	k (10^{-6}cm/s)	32	4.53 (0.08-18.8)
Coefficient of compressibility	$a_{1\text{-}2}$	84	0.95 (0.45-1.74)
Cohesion	c_{cu}/(kPa)	99	9.0 (1.5-18.4)
Internal friction angle	φ_{cu}/(°)	99	16.1 (5.3-30.6)

(a) Stage-loading (SL) test. After the specimen was placed, a sequence of pressures was applied to the specimen with the pressure increment ratio $\Delta p'/p' = 1.0$; the duration of loading was 7 days.

(b) Preloading-stage-loading (pre-SL) test. After the specimen was placed, it was initially preloaded in a surcharge p_e and maintained at this pressure for 24 hours; the pressure was subsequently removed. After the end of rebounding, the SL test was restarted.

(c) Single-loading (SIL) test. The specimen was initially consolidated at a low pressure (such as 6.0 kPa), then subjected to loading in one step and maintained at this pressure for 10-104 days.

Three types of loading methods for the oedometer tests are shown in Fig. 3.

In all tests, the preconsolidation pressure p_c was estimated from the EOP e-lgp' curves using Casagrande's method; the resulting values for the specimens fell in the range of 50-83 kPa. Note that although the preconsolidation pressure denotes the maximum effective vertical stress that previously acted on the clay, the value is difficult to determine as the rate of loading and time has a significant effect on the e-lgp' curve, especially for sensitive structured clays. Burland (1990)

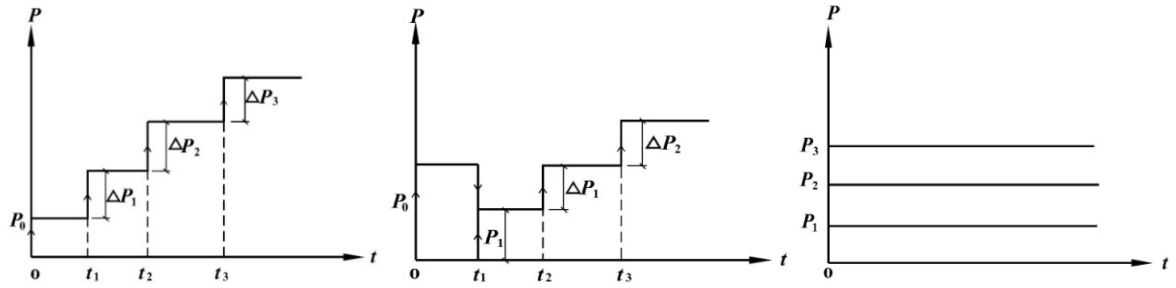

(a) Stage-loading (SL) (b) Preloading-stage-loading (pre-SL) (c) Single-loading (SIL)

Fig. 3 Three types of loading methods for the oedometer test

recommended the use of "yield stress" to replace the traditional term and to describe the critical stress exhibited in the creep process. In this research, p_c is defined as preconsolidation pressure obtained in a standard test with a load increment ratio of 1.0 and a load duration of 24 hours. The test is independent of the previously mentioned types of creep tests.

3.2 Triaxial creep test

In the triaxial creep test, the cylindrical samples were initially split with a fine wire for sub-sampling and trimmed to a diameter of 39.1 mm and a length/diameter ratio of 2. Compared with the conventional strain-controlled triaxial apparatus (the axial stress is indirectly applied by gradually increasing the loading-ram), the triaxial creep tests in this study were performed in a stress-controlled triaxial apparatus. A schematic of the main features of the apparatus, which includes the pressure cylinder, the axial loading, the all-round pressure supply and the drainage, is shown as Fig. 4. The all-round stress and deviator stress are constant in the test, and the values of the axial and/or volumetric strains are directly measured as a function of time.

Two types of creep tests were performed in a stress-controlled triaxial apparatus:

(a) Drained creep test: the drainage of the specimen is permitted under a specified all-round pressure until consolidation is complete. With drainage permitted all time, the increment of deviator stress is applied.

(b) Undrained creep test: the drainage of the specimen is permitted under a specified all-round pressure until consolidation is complete. Then, an increment of deviator stress is applied with no drainage at any stage of loading.

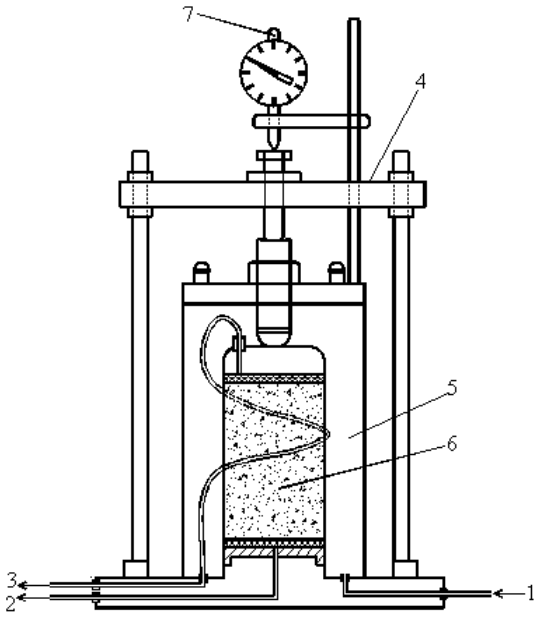

1. All-around pressure supply; 2. Drainage or pore pressure measurement; 3. Top drainage;
4. Axial loading; 5. Pressure cylinder; 6. Soil sample; 7. Displacement measurement

Fig. 4 Schematic of stress-controlled triaxial apparatus

Of all the tests, the duration of each stage deviator stress is determined by the criterion that the axial deformation is less than 0.05 mm/day for a minimum of 72 hours. The applied axial stress q in the creep test can be expressed as the deviator stress level $\overline{D} = q / q_f$, where q_f is the peak of the deviator stress versus the axial strain for a specified all-round pressure, which is obtained by the conventional triaxial test (CIU).

4. Experimental results

4.1 One-dimensional consolidation and secondary consolidation

In the oedometer test, the void ratio e or the vertical strain ε_z are generally plotted versus the logarithm of time t and the vertical effective stress p'. The consolidation and secondary consolidation behaviour in a one-dimensional state can be completely defined by the e-lgp' and e-lg$t$ curves. The e-lg$t$ curve frequently depicts the secondary compression, the slope of one log cycle is defined as the secondary consolidation coefficient $C_\alpha = \Delta e/\Delta \lg t$, and the turning point enotes the time of the end of primary consolidation (refer to Fig. 5). The e-lgp' curves define the compression index $C_C = \Delta e/\Delta \lg p'$.

Fig. 6 shows the measured results of a typical specimen in the SL test, and the initial state of the specimen was $w_0 = 44.2\%$, $e_0 = 1.20$ and $p_c = 50$ kPa. As shown in Fig. 6(a), the e-lgp' curves characteristically depict a reverse "S" in the compression range and are generally parallel in recompression. The duration of the consolidation time does not affect the compressibility index C_c, despite the decrease in the void ratio e with time; the C_c only varies with consolidation pressure. Figs. 6(b)-(c) shows the secondary compression for different consolidation pressures. The curves of e-lg$t$ in the recompression range exhibited approximately linear behaviour. In the compression range, the duration of primary consolidation is extended with decreased p_c/p', and the curve exhibited an indistinct S shape.

Additional test data by SL test, with different natural water contents and void ratios, are plotted in Fig. 7 in terms of C_α-p' (secondary consolidation coefficient versus vertical effective stress) and C_α-C_c (secondary consolidation coefficient versus compression index). C_α was determined from the secondary compression deformation of one log cycle time after the end of primary consolidation $C_\alpha = \Delta e/\Delta \lg t$, and C_c was determined from EOP e-lgp'. In the recompression range, C_α increased

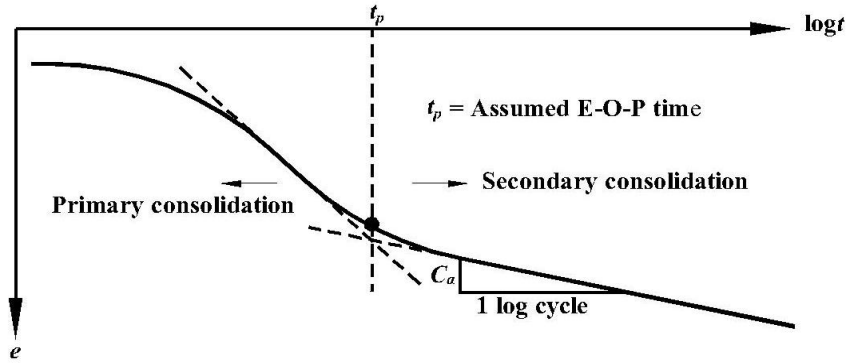

Fig. 5 Idealized relationship of e-lg$t$

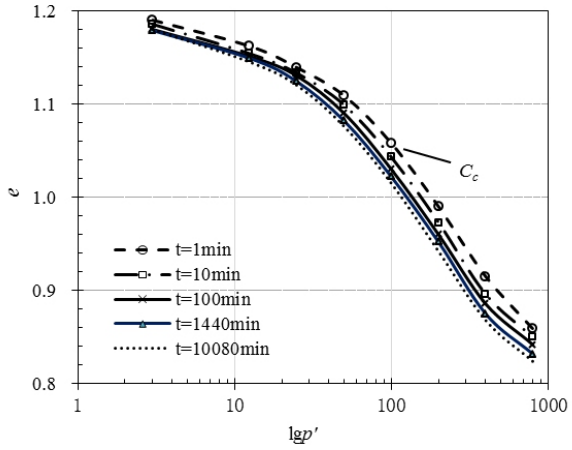

(a) e - lgp'

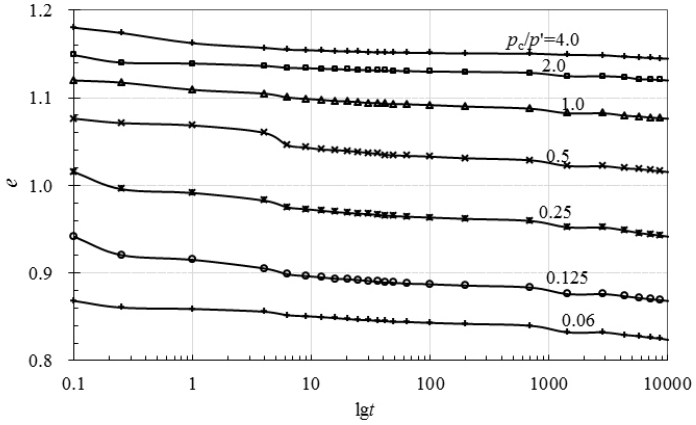

(b) e - lg t

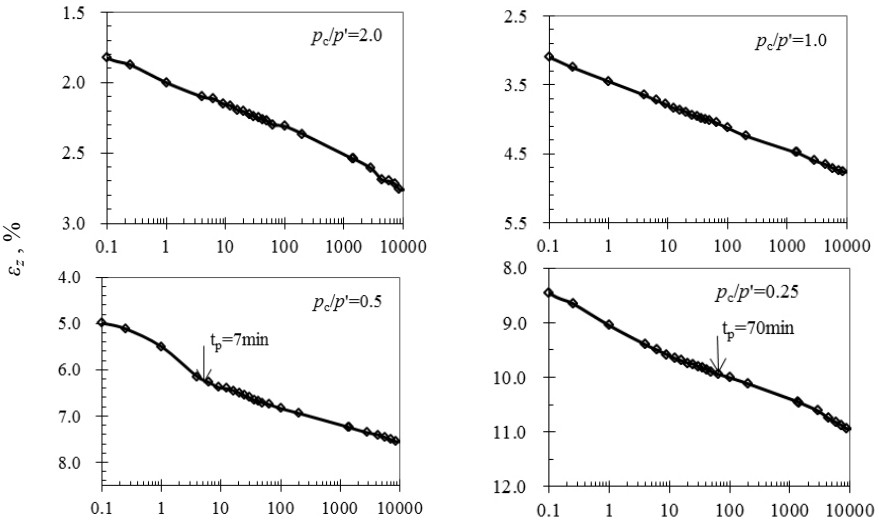

(c) Secondary consolidation for different p_c/p'

Fig. 6 Oedometer tests by the SL test

with consolidation pressure; in the compression range, the value slightly decreased or was constant with consolidation pressure (Fig. 7(a)). The maximum value of C_α generally appeared near p_c, which was also observed in another tests of this clay (Zhou and Chen 2006). As the variations in C_α versus p' correspond to a destruction process of the soil structure, the C_α increase, decrease, or remain constant with the effective vertical stress is dependent on the soil structure. Mesri (Mesri 2003, Mesri and Godlewski 1977, Mesri and Castro 1987, Mesri *et al*. 1997) discovered that a unique interrelationship exists between C_α and C_c throughout the secondary consolidation stage and noted that the C_α/C_c is constant for any soil, that is, soils with high compressibility exhibit high secondary compression, and the magnitude and behaviour of C_α with time directly related to the magnitude and behaviour of C_c with consolidation pressure. As indicated in Fig. 7(b), C_α/C_c = 0.037 for Nansha clay is applicable to the compression and recompression ranges, which is less than general marine clay and has more dispersion than peat deposits.

In practical engineering, surcharging is used to reduce the post-construction secondary settlement of soft ground. In the laboratory pre-SL test, the surcharging process is performed by applying a surcharge p_e on the intact sample, which is higher than p_c. A reloading sequence began after removal of the surcharge and the end of rebounding. Fig. 8 shows the results of a typical sample with w_0 = 47.8%, ρ_0 = 1.68 g/cm^3, e_0 = 1.25 (before preloading) and e_1 = 1.015 (after

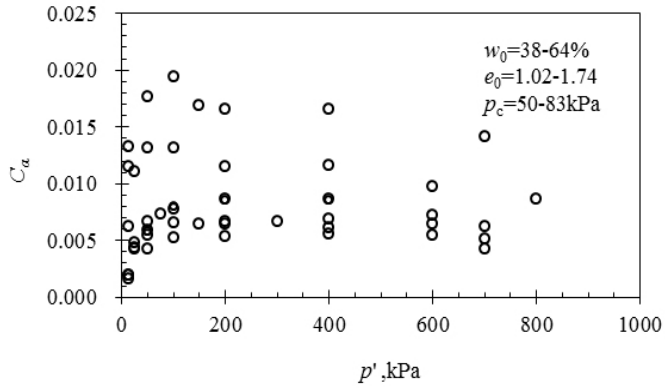

(a) C_α -p'

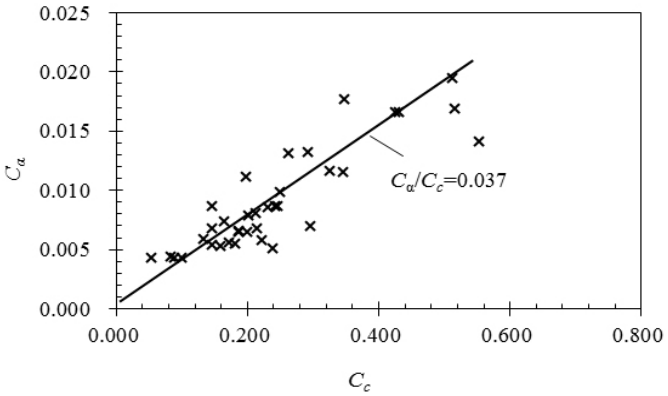

(b) C_α -C_c

Fig. 7 Variation in secondary consolidation coefficient for Nansha clay

rebounded), the p_e = 200 kPa. Obviously, when the sample is preloaded at the surcharge, the initial state of soil changes. Fig. 8(a) shows that the reloading *e*-lg*p′*, curves appear to be merged with time and are linear instead of characteristically concave. Fig. 8(b) reveals that the *e*-lg*t* curves appear to be linear in the recompression range and t_p is very short. In the compression range, the curves exhibit precise bending, and primary and secondary compression can be identified. The slopes of the secondary compression curves slightly decreases or remains constant with time.

Additional data for the pre-SL tests are exhibited in Fig. 9. Fig. 9(a) shows the variation in the postsurcharge secondary consolidation coefficient C_α' with consolidation pressure, which exhibits similar behaviour compared with $C_{\alpha,}$ but the magnitude is significantly smaller. The C_α'/C_c law, which is shown in Fig. 9(b), is a mean constant after removal of the surcharge, which is also lower than C_α/C_c. Note that the difference between C_α'/C_c and C_α/C_c is uncertain and is relevant to the surcharge ratio. As the C_α' is directly proportional to the slopes of the recompression curves until the recompression curve merges with the virgin compression curve, the C_α'/C_c law is predicted by

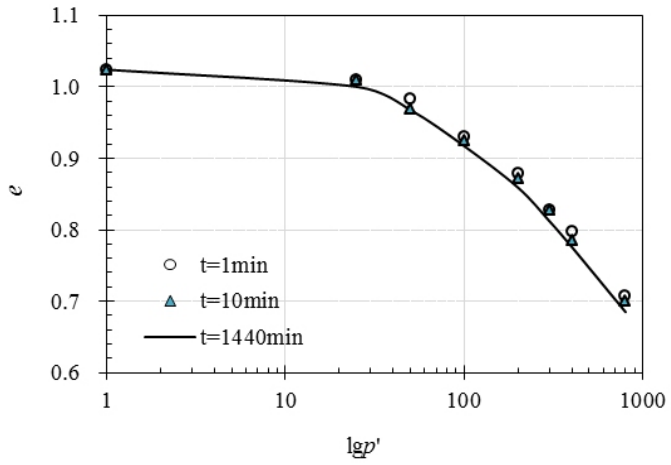

(a) *e* - lg*p′*

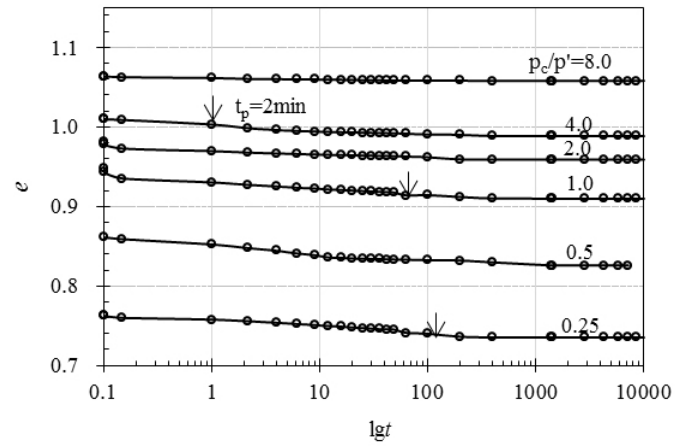

(b) *e* – lg*t*

Fig. 8 Oedometer tests by the pre-SL test

the recompression range. It may be less than or equal to the C_α/C_c of without surcharging (Mesri *et al*. 2001).

The constants of C_α'/C_c =0.028 and C_α/C_c = 0.037 are applicable for with and without surcharging, respectively. Compared with general marine clays, the value of interactive marine and terrestrial clays is lower and more discrete due to its inherent nonuniformity.

Although the stage-loading method is extensively adopted in the laboratory oedometer test, the entire process of creep cannot be obtained due to the continuous compaction of a specimen. Theoretically, the single-loading test (SIL) is a better technique for observing the creep behaviour of soil, however, it is rarely applied due to the difficulty of preparing identical specimens and test conditions.

Fig. 10 shows four typical results from the SIL test. The initial water content was 48.8-57.2% and p_c = 60 kPa. The *e*-lg*t* curves form a typical "S" shape in the normally consolidated case, which differs from the *e*-lg*t* curves in the SL test. The curves are characterized by three compression stages: primary compression, secondary compression in which C_α slightly increases

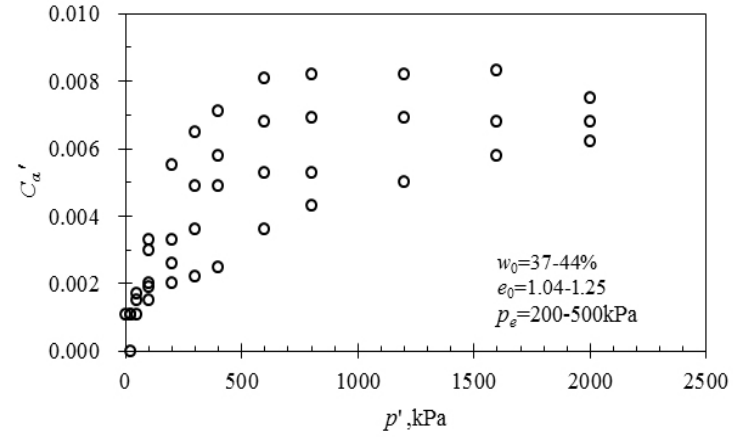

(a) C_α'-p'

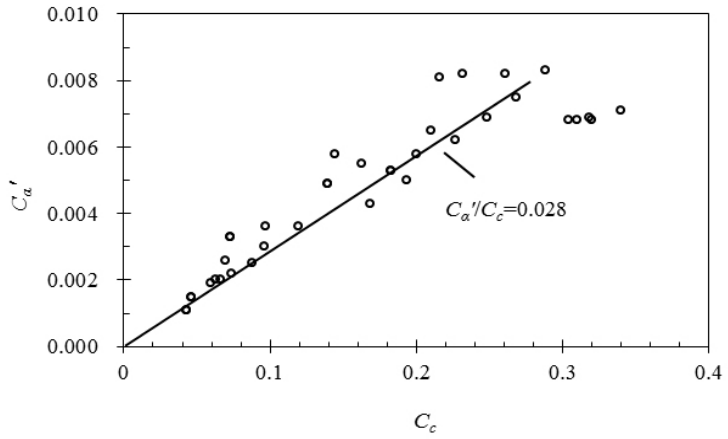

(b) C_α'- C_c

Fig. 9 Postsurcharge variation in secondary consolidation coefficient by the pre-SL test

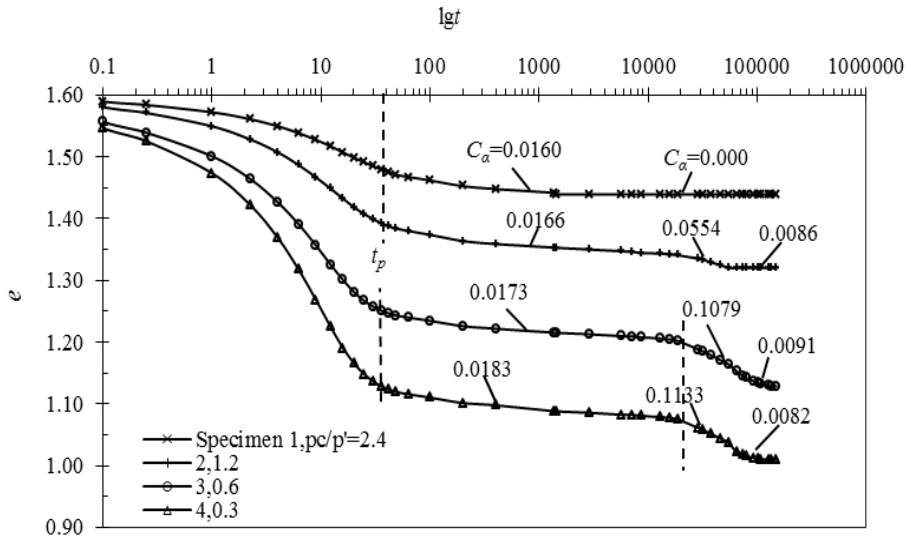

Fig. 10 Oedometer tests by the SIL test

with time, and tertiary compression in which C_α decreases with time. Dhowian and Edil (1980) only observed the relation for the first increment of loading, and den Haan and Edil (1993) defined the tertiary compression. However, the entire process of secondary compression was rarely observed in the stage-loading oedometer creep test. Augustesen *et al*. (2004) even considered that tertiary compression is only an accepted phenomenon for peat. Fig. 10 demonstrates that secondary compression is sustained indefinitely in the normally consolidated case; it began as a linear relation in *e*-lg*t* and followed a steepening curve. The value of C_α was higher than the value obtained in the SL test and varied with time in stages. The duration of primary compression was extended in the recompression and compression range.

Note that the concept of C_α/C_c is indistinct in the SIL test as the *e*-lg*p′* curves were obtained from different specimens, which do not correspond with the definition of the compression index C_c.

4.2 Triaxial compression creep

In the triaxial compression creep test, the samples were consolidated under all-round pressure σ_3 firstly, then subjected to a sequence of deviator stress q with drainage either permitted or not permitted. Fig. 11 shows the entire process curves of axial strain ε_z during drained creep and undrained creep of two typical samples, with an initial strength q_f of 200 kPa for a drained specimen, an initial strength of 120 kPa for an undrained specimen and w_0 = 64.6% and w_0 = 66.6%, respectively. As indicated in Fig. 11, the instantaneous strain is distinct at the first deviator stress level and the second deviator stress level (only in drained). With the application of deviator stress increments, ε_z gradually increases with time and is smaller for the undrained creep compared with drained creep. In the undrained creep test, the creep failure is observed at a high stress level as the undrained creep can cause long-term strength reductions.

Note that the creep state varies during the drained and undrained tests. In the drained creep test,

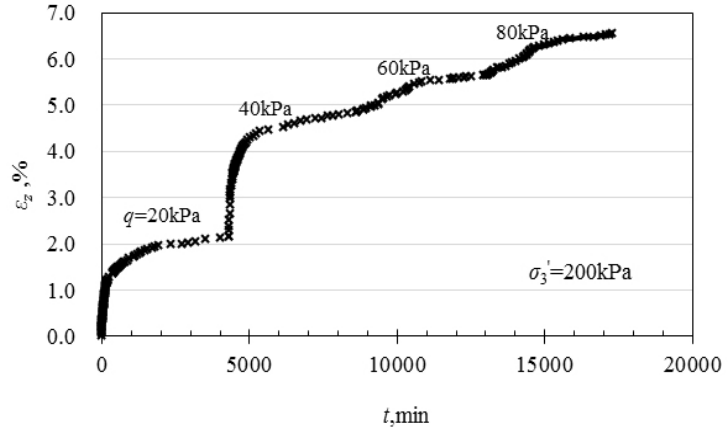

(a) Drained creep

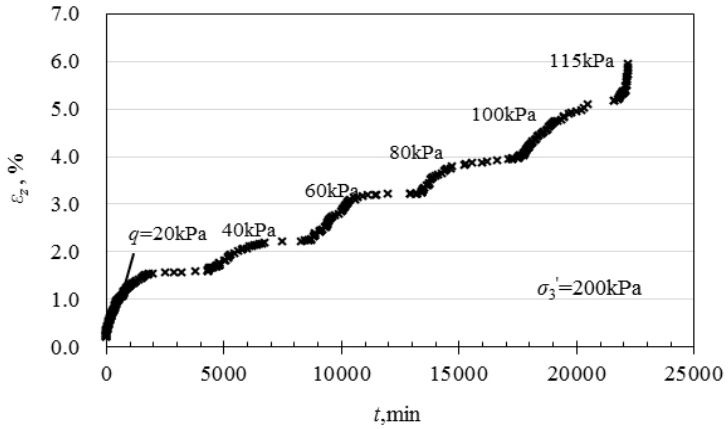

(b) Undrained creep

Fig. 11 The entire process curve for the triaxial creep test

the effective mean stress p' and the deviator stress q are constant, and the creep behavior is governed by the volumetric creep rate and the consolidation rate. In the undrained creep test, the drains are closed and the effective mean stress p' decreased with increasing pore pressure, and the behaviour is controlled by the shear creep rate and the loading rate (in the process, q is independent of pore pressure and remains constant). Therefore, the time-dependent deformation in the triaxial creep test is influenced by the interaction consolidation and creep. The undrained creep does not represent a pure creep process for the varied effective stress p'. As no volumetric strain exists in the undrained condition, the axial strain is shear creep, which increases with time. When q = 115 kPa, which is less than the peak stress q_f (measured in a CIU test), the creep rapidly increases with time and the sample failed in creep rupture mode after a few hours. The failure is related to the reduction in strength with the rapid increase in pore pressure during the stress state.

The creep test data are plotted in the logarithm of the axial strain rate and time diagrams, as shown in Fig. 12. The $\lg \dot{\varepsilon}_z$ decreases linearly with lg$t$ in the drained and undrained conditions (with the exception of the first increment q = 20 kPa), and the slope of $\lg \dot{\varepsilon}_z - \lg t$ diagram is

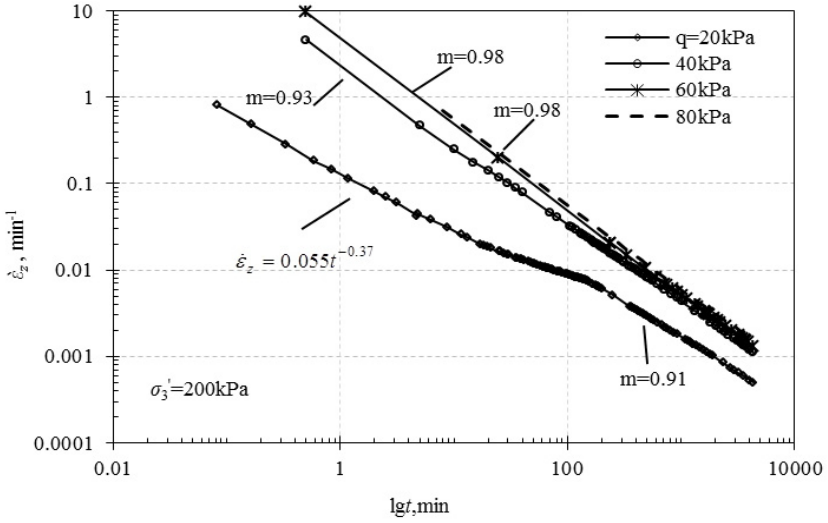

(a) Drained creep

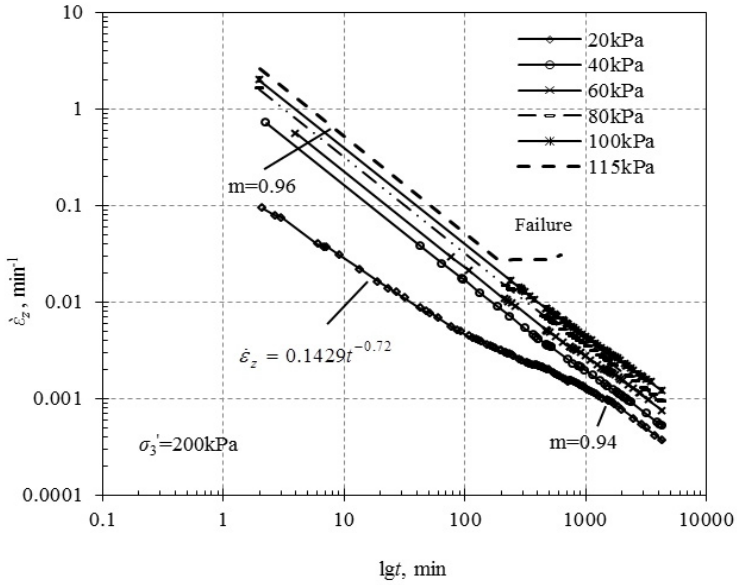

(b) Undrained creep

Fig. 12 Axial strain rate $\lg \dot{\varepsilon}_z$ versus lg*t* relationship of Nansha clay

characterized by the *m* parameter (Singh and Mitchell 1968).

$$m = \Delta \lg \dot{\varepsilon}_z / \Delta \lg t \tag{1}$$

According to Fig. 12(a), when the applied deviator stress ranges from 40 kPa to 80 kPa, *m* slightly increases and approaching a constant value (approximately *m* = 1.0). In Fig. 12(b), *m* is independent of the deviator stress level range from 40 kPa to 100 kPa with a value of 0.96. These

values are higher than the values for marine clay and peat. Affected by instantaneous compression in the test, the strain rate behaviour in the first deviator stress level is characterized as bilinear (refer q = 20 kPa diagram); it converged in approximately 130 min for drained creep and converged in approximately 400 min for undrained creep. Based on the plot, a power relation between the creep strain rate and time may be more appropriate, which are marked in Figs. 12(a)-(b).

According to Singh and Mitchell (1968), the relationship among creep strain rate, deviator stress level and time can be expressed as

$$\dot{\varepsilon} = Ae^{\alpha\overline{D}}\left(\frac{t_1}{t}\right)^m \tag{2}$$

where α and A are soil parameters, $\overline{D}$ is the deviator stress level, t_1 is the reference time (1 min, 1 h, 1 d, and so on), and m is the slope of the $\lg\dot{\varepsilon}_z - \lg t$ curves.

From the data obtained from the tests, the parameters can be determined by $\lg\varepsilon_z =$

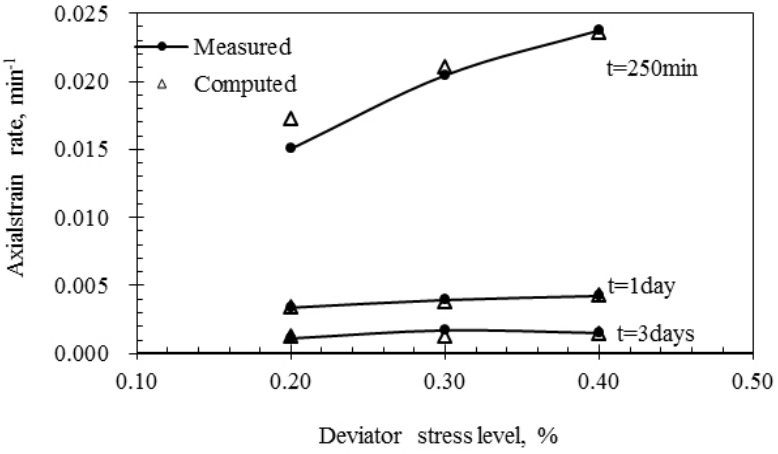

(a) Drained creep

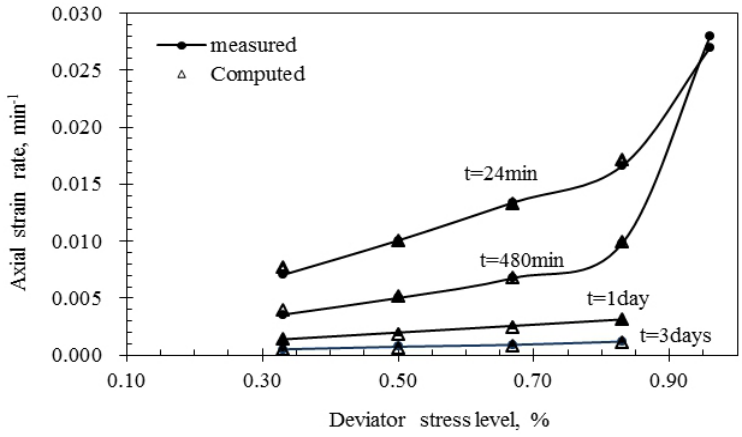

(b) Undrained creep

Fig. 13 Axial strain rate versus deviator stress level

$\alpha\overline{D} + \ln\dfrac{At_1}{1-m}$ based on the diagram of logarithm creep strain and deviator stress level. For t_1 = 1d = 1440 min, Eq. (2) may be expressed as follows (m shown in Fig. 12)

$$\text{Drained creep} \qquad \dot{\varepsilon} = 0.0027e^{1.129\overline{D}}\left(\frac{t_1}{t}\right)^m \qquad (\overline{D} = 0.2; 0.3; 0.4) \tag{3}$$

$$\text{Undrained creep} \qquad \dot{\varepsilon} = 0.0008e^{0.0135\overline{D}}\left(\frac{t_1}{t}\right)^m \qquad (\overline{D} = 0.33; 0.5; 0.67; 0.83) \tag{4}$$

Fig. 13 shows the variation in the axial strain rate $\dot{\varepsilon}_z$ with the deviator stress level $\overline{D}$ for different creep times. The comparison of measured and computed creep behaviours shows that the strain rate concept of m can accurately predict creep in a given range of deviator stress level. Fig. 13 reveals that the development of creep is closely related to the drainage conditions and the deviator stress level. For the drained test, the initial strain rate is distinct at low stress levels, followed by an increases with the deviator stress, and tend to a small constant rate as time increases (refer to Fig. 13(a)). During undrained creep (Fig. 13(b)), an increased deviator stress level resulted in an increased creep rate. When the deviator stress approaches the initial strength of the soil, the strain rate increases and signals a failure. The measured data showed that the failure occurred at $\overline{D} = 0.95$, which was beyond the applicable range of Eq. (2).

5. Conclusions

A series of oedometer tests and triaxial creep tests were performed on Nansha clay to investigate the time-dependent deformation behavior.

- Normally consolidated soils exhibit larger secondary compression compared with overconsolidated soils, and the maximum value of the secondary consolidation coefficient C_α generally appears in the vicinity of the preconsolidation pressure. The postsurcharge C_α' is significantly less than C_α.
- The observed secondary compression behaviour is consistent with the C_α/C_c concept, regardless of surcharging. The C_α/C_c ratio is a constant that is applicable to the recompression and compression ranges, which are 0.037 for C_α/C_c and 0.028 for C_α'/C_c. They are lower compared with marine clays.
- In the single-loading oedometer test, the entire process of secondary compression can be observed, which is characterized by three compression stages: primary compression, secondary compression and tertiary compression. The e-lg$t$ curve exhibits a steepening shape. C_α significantly varies with time, and the value is larger than the value obtained in the stage-loading oedometer test.
- The creep state is different in the drained and undrained triaxial creep tests, which is governed by the volumetric creep rate and the consolidation rate in the drained creep tests and is controlled by the shear creep rate and the loading rate in the undrained triaxial creep tests.
- The axial creep strain gradually increases with time, and the behaviour can be analyzed by a characteristic relationship between the logarithm of strain rate and the logarithm of time. The

slope of $\lg \dot{\varepsilon}_z / \Delta \lg t$ is independent of deviator stress level (with the exception of the first stage increment), which ranges from 0.93-0.98 for the drained case and 0.96 for the undrained case. The typical formula for the relationships among axial strain rate, deviator stress level and time can accurately predict the creep of clay for a given deviator stress level range.

Acknowledgments

This research was sponsored by the National Natural Science Foundation of China (Grant No. 41472279) and the Guangdong Provincial Water Resources Science & Technology Project (Grant No. 201104).

References

Al-Shamrani, M. (1998), "Application of the C_α/C_c concept to secondary compression of Sabkha soils", *Can. Geotech. J.*, **35**(1), 15-26.

Arulanandan, K., Shen, C.K. and Young, R.B. (1971), "Undrained creep behaviour of a coastal organic silty clay", *Geotechnique*, **21**(4), 359-375.

Augustesen, A., Liingaard, M. and Lade, P.V. (2004), "Evaluation of time-dependent behavior of soils", *Int. J. Geomech.*, **4**(3), 137-156.

Badv, K. and Sayadian, T. (2012), "An investigation into the geotechnical characteristics of Urmia peat", *Iran. J. Sci. Tech.-Transact. Civil Eng.*, **36**(C2), 167-180.

Bishop, A.W. and Lovenbury, H.T. (1969), "Creep characteristics of two undisturbed clays", *Proceedings of 7th International Conference of Soil Mechanics and Foundation Engineering*, Mexico, 1, 29-37.

Burland, J.B. (1990), "On the compressibility and shear strength of natural clays", *Géotechnique*, **40**(3), 329-378.

Chen, X.P., Zeng, L.L., Lü, J., Qian, H. and Kuang, L.W. (2008), "Experiment study of mechanical behavior of structured clay", *Chin. J. Rock Soil Mech.*, **29**(12), 3223-3228.

Deng, Y.F., Cui, Y.J., Tang, A.M., Li, X.L. and Sillen, X. (2012), "An experimental study on the secondary deformation of boom clay", *Appl. Clay Sci.*, **59-60**, 19-25.

den Haan, E.J. and Edil, T.B. (1993), "Secondary and tertiary compression of peat", *Proceedings of the International Workshop on Advances in Understanding and Modelling the Mechanical Behaviour of Peat*, Rotterdam, Netherlands, June.

Dhowian, A.W. and Edil, T.B. (1980), "Consolidation behavior of peats", *Geotech. Test. J.*, **3**(3), 105-114.

Fodil, A., Aloulou, W. and Hicher, P.Y. (1997), "Viscoplastic behavior of soft clay", *Geotechnique*, **47**(3), 581-591.

Jesmani, M., Vaezi, R. and Kamalzare, M. (2012), "Correlation between C_α/C_c ratio and index parameters of soil", *Quarter. J. Eng. Geol. Hydrogeol.*, **45**(2), 207-220.

Mesri, G. (1973), "Coefficient of secondary compression", *J. Soil Mech. Found. Div.*, *ASCE*, **99**(1), 123-137.

Mesri, G. (2003), "Primary compression and secondary compression", *Geotech. Spec. Pub.*, **119**, 122-166.

Mesri, G. and Castro, A. (1987), "C_α/C_c concept and K0 during secondary compression", *J. Geotech. Eng.*, *ASCE* , **113**(3), 230-247.

Mesri, G. and Godlewski, P.M. (1977), "Time and stress compressibility interrelationship", *J. Geotech. Eng. Div.*, *ASCE*, **103**(5), 417-430.

Mesri, G., Stark, T.D., Ajlouni, M.A. and Chen, C.S. (1997), "Secondary compression of peat with or without surcharging", *J Geotech. Geoenviron. Eng.*, **123**(5), 411-421.

Mesri, G., Ajlouni, M.A., Feng, T.W. and Lo, D.O.K. (2001), "Surcharging of soft ground to reduce

sencondary compression", *Proceedings of 3th International Conference on Soft Soil Engineering*, Hong Kong, December, pp. 55-65.
Miao, L., Zhang, J. and Wang, F. (2008), "Time-dependent deformation behavior of Jiangsu marine clay", *Marine Georesour. Geotechnol*., **26**(2), 86-100.
Qiao, J.G., Huang, Z.G. and Huang, G.Q. (2002), "The mollisol layers digital terrain model of the Pearl River delta", *Chin. J. Foshan Univ*. (*Natural Science Edition*), **20**(4), 47 -52.
Santagata, M., Bobet, A., Johnston, C.T. and Hwang, J. (2008), "One-dimensional compression behavior of a soil with high organic matter content", *J. Geotech. Geoenviron*., **134**(1), 1-13.
Sheahan, T., Ladd, C. and Germaine, J. (1996), "Rate-dependent undrained shear behavior of saturated clay", *J. Geotech. Eng*., **122**(2), 99-108.
Singh, A. and Mitchell, J.K. (1968), "General stress-strain-time function for soils", *J. Soil Mech. Found. Div*., **94**(1), 21-46.
Tavenas, F., Leroueil, S., La Rochelle, P. and Roy, M. (1978), "Creep behaviour of an undisturbed lightly overconsolidated clay", *Can. Geotech. J*., **15**(3), 402-423.
Tian, W.M., Silva, A.J., Veyera, G.E. and Sadd, M.H., (1994), "Drained creep of undisturbed cohesive marine sediments", *Can. Geotech. J*., **31**(6), 841-855.
Tong, F., Yin, J.H. and Pei, H.F. (2012), "Experimental study on complete consolidation behavior of Hong Kong marine deposits", *Marine Georesour. Geotechnol*., **30**(4), 291-304.
Zeng, L.L. and Chen, X.P. (2009), "Analysis of mechanical characteristics of soft soil under different stress paths", *Chin. J. Rock Soil Mech*., **30**(5), 1264-1270.
Zhou, Q.J. and Chen, X.P. (2006), "Experimental study on creep characteristics of soft soils", *Chin. J. Geotech. Eng*., **28**(5), 626-630.
Zhu, J.G. and Yin, J.H. (2001), "Drained creep behaviour of soft Hong Kong marine deposits", *Geotechnique*, **51**(5), 471-474.

CC